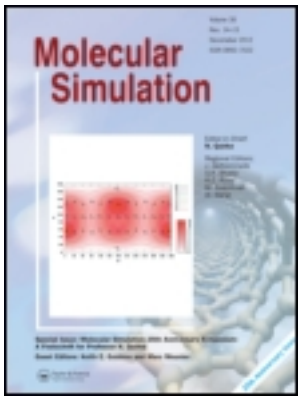

Molecular Simulation
Publication details, including instructions for authors and subscription information:
http://www.tandfonline.com/loi/gmos20

Top-leads from natural products for treatment of Alzheimer's disease: docking and molecular dynamics study

Son Tung Ngo [a] & Mai Suan Li [b]

[a] Institute for Computational Science and Technology, 6 Quarter, Linh Trung Ward, Thu Duc District, Ho Chi Minh City, Vietnam

[b] Institute of Physics, Polish Academy of Sciences, Al. Lotnikow 32/46, 02-668, Warsaw, Poland

Version of record first published: 10 Oct 2012.

To cite this article: Son Tung Ngo & Mai Suan Li (2013): Top-leads from natural products for treatment of Alzheimer's disease: docking and molecular dynamics study, Molecular Simulation, 39:4, 279-291

To link to this article: http://dx.doi.org/10.1080/08927022.2012.718769

Molecular Simulation, 2013
Vol. 39, No. 4, 279–291, http://dx.doi.org/10.1080/08927022.2012.718769

Taylor & Francis
Taylor & Francis Group

Top-leads from natural products for treatment of Alzheimer's disease: docking and molecular dynamics study

Son Tung Ngo[a] and Mai Suan Li[b]*

[a]*Institute for Computational Science and Technology, 6 Quarter, Linh Trung Ward, Thu Duc District, Ho Chi Minh City, Vietnam;* [b]*Institute of Physics, Polish Academy of Sciences, Al. Lotnikow 32/46, 02-668 Warsaw, Poland*

(*Received 31 October 2011; final version received 2 August 2012*)

Since available drugs are not efficient to treat Alzheimer's disease (AD), the search for new leads is of great interest. One of possible ways is to use the Eastern medicine. Because the aggregation of amyloid peptides $A\beta_{1-40}$ and $A\beta_{1-42}$ may be responsible for AD, we have collected 342 compounds derived from Vietnamese plants and studied their binding affinity to these peptides and their mature fibrils using the docking technique combined with the molecular mechanic-Poisson–Boltzmann surface area method. We predict that five ligands Dracorubin, Taraxerol, Taraxasterol, Hinokiflavone and Diosgenin, showing high-binding affinity to monomers and mature fibrils of amyloid peptides, may be good candidates to cope with AD. Dracorubin and Taraxerol are eventually more promising than Curcumin (diferulom-rthane) which is under clinical trial. Five top-leads can cross the blood–brain barrier as well as be well absorbed by human body.

Keywords: Alzheimer; herbs; drug design; docking; MM-PBSA

1. Introduction

Alzheimer's disease (AD) is the most common late-life neurodegenerative disorder that affects approximately 36 million people worldwide as of 2009 [1]. Currently, five drugs, Donepezil, Galantamine, Rivastigmine, Tacrine and Memantine, are prescribed for symptomatic treatments. The first four medicines are acetylcholinesterase inhibitors, whereas Memantine modulates N-methyl-D-aspartic acid. Doctors rarely prescribe Tacrine today because it is associated with more serious side effects than the other drugs. Since all of the drugs do not actually slow down or reverse the progression of the disease, the search for new leads is of great interest.

There is an enormous amount of evidence that AD is associated with oligomerisation of beta amyloid (Aβ) peptides [1]. From this point of view, one of the strategies to cope with this disease is to find compounds that are able to promote Aβ anti-aggregation and clearance. Because Aβ is self-assembling, such a strategy may be realised by using short peptide fragments homologous to the full-length wild-type protein [2–6] or N-methylated peptides [7] as inhibitors [8]. Carbohydrate-containing compounds, polyamines, chaperones, metal chelators, etc. may be used to interfere with Aβ fibrillogenesis (see recent reviews [9,10]). Nutraceuticals which are natural products or extracts therefrom, as shown by preclinical and certain clinical studies, may be of value as AD therapy [11,12]. Among them, Curcumin (diferulom-rthane) [13], ginkgo biloba [14] and (−)-epigallocatechin-3-gallate (EGCG; green tea) [15] from the traditional Chinese and Indian medicines are reported to inhibit Aβ aggregation and as antidotes of Aβ-induced toxicity. Clinical trials are going in phases II and III for Curcumin [16] and ginkgo biloba [17], respectively.

Although the traditional Vietnamese medicine shares common features with Chinese and Indian medicines, it has many specific herbs due to difference in geography and soil quality [18]. Thus, it is worth to search among Vietnamese herbs possible leads for anti-aggregation of amyloid peptides. In this study, we have collected 342 compounds derived from Vietnamese plants and studied their binding affinity to full-length $A\beta_{1-40}$ and $A\beta_{1-42}$ peptides and their mature fibrils using the Autodock Vina version 1.1 [19] and molecular dynamics (MD) simulations. For mature fibrils we have considered twofold symmetry structures derived by the Tycko group for hexamer of truncated peptides $A\beta_{9-40}$ ($6A\beta_{9-40}$) [20,21] and pentamer of $A\beta_{17-42}$ fragment ($5A\beta_{17-42}$) by the Luhrs group [22]. Top-leads found by the docking technique are further refined by the more accurate molecular mechanic-Poisson–Boltzmann surface area (MM-PBSA) method.

It has been shown that four sets of binding energies to four targets β_{1-40}, $A\beta_{1-42}$, $6A\beta_{9-40}$ and $5A\beta_{17-42}$ are highly correlated with each other. A detailed analysis of the nature of ligand binding reveals that together with hydrogen bonds (HBs), the electrostatic and van der Waals (vdW) interactions also play an important role. Based on the results obtained by the docking and MM-PBSA methods, we predict that five ligands Dracorubin, Taraxerol, Taraxasterol,

*Corresponding author. Email: masli@ifpan.edu.pl

Hinokiflavone and Diosgenin are good candidates for treating AD.

For designing oral drugs for AD, it is important to know whether they can pass the blood–brain barrier (BBB) and be absorbed by the human body. We have computed log (BB) (see Equation (1)) and the human intestinal absorption (HIA) [23] using the PreADME software [24] and shown that five top-leads fulfil these requirements for AD drugs having high values of log(BB) and HIA. Their toxicity and metabolism are also analysed.

2. Materials and methods

2.1 Set of receptor–ligand complexes

We consider four receptors including monomers $A\beta_{1-40}$ and $A\beta_{1-42}$ and protofibrils of their fragments $6A\beta_{9-40}$ and $5A\beta_{17-42}$ (first 8 and 16 unstructured amino acids re-excluded from mature fibrils). The NMR structures of $A\beta_{1-40}$ [Protein Data Bank (PDB) ID: 1BA4 [25]] and $A\beta_{1-42}$ (PDB ID: 1Z0Q [26]) peptides were taken from the PDB. Coordinates of twofold symmetry $6A\beta_{9-40}$ were provided by Tycko [21], whereas the crystal structure of $5A\beta_{17-42}$ was taken from the PDB (PDB ID: 2BEG [22]). 1BA4 and 2BEG have 10 models whereas 1Z0Q has 30 models. For docking simulation, we have chosen their first model.

The ligands set contains 342 compounds derived from Vietnamese herbs [18], but their chemical structures are known from the Pubchem and Chemspider database (see http://pubchem.ncbi.nlm.nih.gov and http://www.chemspider.com/). The general Assisted Model Building with Energy Refinement (AMBER) force field [27] has been used to generate ligand parameters except for charges, which came from Molecular Orbital PACkage (MOPAC) using the Austin model 1-bond charge correction (AM1-BCC) [28]. This procedure was done by Ambertools-1.4.

2.2 Docking

In docking of ligands to full-length Aβ peptides and their fibrils, we prepare PDBQT file for receptor and ligand using AutodockTools 1.5.4 [29]. The Autodock Vina version 1.1 [19], which is much more efficient than Autodock 4, was used. Atomic interactions are described by a modified version of the Chemistry at HARvard Molecular Mechanics (CHARMM) force field [30,31]. In the Autodock Vina software, the Broyden–Fletcher–Goldfarb–Shanno method [32] is implemented for local optimisation. To obtain reliable results, the exhaustiveness of global search was set equal to 400 whereas the maximum energy difference between the best and worst binding modes is chosen to be 7. Twenty modes of docking were generated with random starting positions of ligand which has fully flexible torsion degrees of freedom. Positions of all atoms of the receptor are kept fixed. The centre of grids is placed at the centre of mass of receptor and grid dimensions were chosen large enough ($60\times 50\times 50$, $70\times 50\times 50$, $90\times 70\times 50$ and $80\times 60\times 60$ Å for $A\beta_{40}$, $A\beta_{42}$, $6A\beta_{9-40}$ and $5A\beta_{17-42}$, respectively) to cover all parts of the receptor.

2.3 BBB and HIA

The BBB is a physical barrier in the circulatory system that compounds must cross in order to travel into the central nervous area [33]. Thus, the requirement of passing this barrier is necessary for any AD drug candidate. The crossing ability through the BBB is measured by the logarithm base 10 of the ratio of the compound concentration in the brain, C_{brain}, to that in the blood, C_{blood}:

$$\log(\text{BB}) = \log\left[\frac{C_{\text{brain}}}{C_{\text{blood}}}\right]. \quad (1)$$

BB is likely related to local hydrophobicity, molecular size, lipophilicity and molecular flexibility [34]. In this study, BB is computed using the quantitative structure–activity relationship (QSAR) model [33,35] implemented in the PreADME prediction software [36]. This method was proved to provide estimations highly correlated with experimental data [35].

Another important aspect of the oral drug design is HIA [23] which measures drug percentage that can be absorbed by the human body. HIA should be high enough for drug efficacy. According to 'rule of 5' [36,37], it depends on molecular weight, number of HB donors, number of HB acceptors, $C\log P$ and $M\log P$. HIA of all compounds is estimated by the QSAR method [23,36,38,39] which is also implemented in the PreADME suit [36].

2.4 Molecular dynamic simulations

We have used AMBER 10 package [40] to run MD simulations with the AMBER 99SB force field. The water model TIP3P [41] was chosen following the recommendation of this package. Nine complexes of $6A\beta_{9-40}$-ligand were placed in a triclinic box of about 9500 water molecules with 0.7 nm distance between the solute and box. The typical initial conformation is shown in Figure S1 in supporting information (SI), online only, $6A\beta_{9-40}$ has 2862 atoms, whereas Dracorubin, Solasodine, Taraxasterol, Amentoflavone, Hinokiflavone, Kulolactone, Hecogenin, Taraxerol and Diosgenin, respectively, have 61, 74, 81, 58, 58, 79, 73, 81 and 72 atoms (see below). To neutralise systems, six Na^+ ions were added (Figure S1), except for the complex with ligand Solasodine into which five Na^+ ions were added.

The long-range electrostatic interaction is computed by particle-mesh Ewald summation method [42]. Equations of motion were integrated using a leap-frog

algorithm [43] with a time step 2 fs. The non-bonded interaction pair-list was updated every 10 fs with the cut-off of 0.8 nm. The systems were minimised to remove bad vdW contacts with water. Then the temperature was gradually increased from 0 to 300 K for 50 ps. For density equilibration, MD simulation was carried out with weak restraints on all bonds of the complex for 50 ps at constant temperature, 300 K [44,45]. Restraints have been implemented by the linear constraint solver (LINCS) algorithm [46]. Constant temperature 300 K was enforced using Berendsen algorithm [47] under 500 ps canonical ensemble (NVT) simulation with a damping coefficient of 0.1 ps. The final MD simulation was carried out in the isothermal-isobaric (NPT) ensemble using Parrinello–Rahman pressure coupling [48] at 1 atm with the damping coefficient of 0.5 ps.

2.5 Binding free energy calculation by MM-PBSA

The binding free energy is defined as follows:

$$\Delta G_{\text{bind}} = G_{\text{complex}} - G_{\text{free-protein}} - G_{\text{free-ligand}}. \quad (2)$$

In the MM-PBSA, the free energy of each molecule is given by the following equation:

$$G = E_{\text{mm}} + G_{\text{solvation}} - TS. \quad (3)$$

The molecular mechanics energy of the solute in the gas phase E_{mm} includes bond, bond-angle, dihedral-angle, electrostatic and vdW (Lennard-Jones) terms:

$$E_{\text{mm}} = E_{\text{bond}} + E_{\text{angle}} + E_{\text{torsion}} + E_{\text{elec}} + E_{\text{vdW}}. \quad (4)$$

To incorporate all possible non-bonded interactions, E_{mm} was computed without cut-off utilising AMBER tool.

The free energy of solvation, $G_{\text{solvation}}$, was approximated as the sum of electrostatic and non-polar contributions,

$$G_{\text{solvation}} = G_{\text{PB}} + G_{\text{sur}}. \quad (5)$$

Here G_{PB} derived from the electrostatic potential between solute and solvent was determined using the continuum solvent approximation [49]. It is the change of electrostatic energy from transferring solute in a continuum medium, from a low solute dielectric constant region ($\varepsilon = 2$) to higher one with water without salt ($\varepsilon = 78.45$). Using grid spacing 0.1 Å, the APBS package [50] was implemented for numerical solution of the corresponding linear Poisson–Boltzmann equation. The GROMOS radii and charges were used to generate PQR files. Then the non-polar solvation term G_{sur} was approximated as linearly dependent on the solvent-accessible surface area (SASA), derived from Shrake–Rupley numerical method [51] integrated in the APBS package. $G_{\text{sur}} = \gamma\text{SASA} + \beta$, where $\gamma = 0.0072$ kcal/mol Å^2 and $\beta = 0$ [52].

Solute entropy contributions were estimated from the structures obtained in the equilibrium. In the MM-PBSA method, the conformational entropy of the solute is approximated by the vibrational entropy S_{vib} that is estimated from normal mode analysis by diagonalising the mass-weighted Hessian matrix [53] as follows:

$$S_{\text{vib}} = -R \ln\left(1 - \mathrm{e}^{-h\nu_0/k_{\text{B}}T}\right) + \frac{N_{\text{A}}\, \nu_0 \mathrm{e}^{-h\nu_0/k_{\text{B}}T}}{T\left(1 - \mathrm{e}^{-h\nu_0/k_{\text{B}}T}\right)}, \quad (6)$$

where h is Plank's constant, ν_0 the frequency of the normal mode, k_{B} the Boltzmann constant, $T = 300$ K and N_{A} Avogadro's number. We used snapshots collected every 10 ps in the equilibrium to compute other terms of ΔG_{bind}.

2.6 Measures used in data analysis

The backbone root mean square deviation (RMSD) is used to measure the deviation of structures of the receptor from its initial configuration. The HB is assumed to be formed if the distance between proton donor (D) and proton acceptor (A) is < 0.35 nm and the angle H–D–A is also $< 30°$. The time evolution of formation of contacts between side chain (SC) of receptor and the ligand is also monitored. SC contact is formed if the distance between the centres of mass of the ligand and receptor is ≤ 6.5 Å.

3. Results and discussion

3.1 Human intestinal absorption

Having used the PreADME prediction software [36], we calculated HIA for 342 compounds (Figure S2 and Table S1). This value varies between 0% and 100% but its average value is very high (81%), implying that most of ligands can be absorbed by the human body. Among them 50 compounds have HIA equal to 100%, and 227 compounds have HIA $> 90\%$. Only six ligands are not able to penetrate the body having HIA $= 0$. Curcumin which is a potential drug for treating AD has high HIA of 94%, whereas other candidates have relatively low absorption ability. For instance, HIA = 65%, 40%, 21%, 40% and 21% for Ginkgolide A, Ginkgolide B, Ginkgolide C, Ginkgolide J and EGCG, respectively (Table S1 in SI, online only). Thus, most of the ligands display higher absorption ability than leads that are under intensive clinical trial.

3.2 Blood–brain barrier

Since amyloid peptides are located in the brain, an efficient drug should be able to cross the BBB to interfere their activity. Using the PreADME prediction method, we have calculated log(BB) (Equation (1)) which measures a percentage of drug that can permeate the brain. The results obtained for all compounds are shown on Table S1 in SI.

Experimental values of log(BB) of drugs published to date cover the range between -2.0 and $+1.0$ [36].

Compounds with log(BB) > 0.3 can cross the BBB easily, whereas compounds with log(BB) < -1.0 are poorly distributed in the brain [36]. As seen from Table S1, the average value of log(BB) is -0.31. Compound Taraxasterol has the largest penetration ability log(BB) $= 1.36$, whereas ligand 10,607 has the smallest penetration ability log(BB) $= -2.0$. We found 91 compounds with log(BB) < -1.0 and 24 compounds that have log(BB) larger than 1.00. At least 227 compounds can pass through the BBB easily. There is weak correlation between HIA and log(BB) with the correlation level $R = 0.54$ (Figure S2 in SI, online only).

3.3 *Docking results*

3.3.1 *Binding energies: correlation between four sets*

Having used the Autodock Vina version 1.1 [19], we carried out docking of 342 ligands to $A\beta_{1-40}$, $6A\beta_{9-40}$, $A\beta_{1-42}$ and $5A\beta_{17-42}$. For each receptor E_{bind} obtained from the best mode are listed in Table S1 in SI. The second column refers to ID of ligands according to the Pubchem and Chemspider database (see http://pubchem.ncbi.nlm.nih.gov and http://www.chemspider.com/). The distributions of E_{bind} for four sets are shown in Figure 1. Ligands showing the highest binding affinity to $6A\beta_{9-40}$ have $-3.1 \le E_{bind} \le -9.8$ kcal/mol, whereas $-3.1 \le E_{bind} \le -8.9$, $-2.7 \le E_{bind} \le -8.4$ and $-3.4 \le E_{bind} \le -8.1$ kcal/mol are for $A\beta_{1-40}$, $A\beta_{1-40}$ and $5A\beta_{17-42}$ (Figure 1 and Table S1), respectively. The average of binding energies of ligands to $6A\beta_{9-40}$, $5A\beta_{17-42}$, $A\beta_{1-40}$ and $A\beta_{1-42}$ is -6.6, -6.2, -5.9 and -5.5 kcal/mol, respectively.

Two sets of binding energies to fibril $6A\beta_{9-40}$ and monomer $A\beta_{1-40}$ display high correlation with the correlation level $R = 0.91$ (Figure 2). In the case of the longer 42-bead peptide, the correlation level drops to $R = 0.78$ for targets $A\beta_{1-42}$ and $5A\beta_{17-42}$ (Figure S3 in SI). For the remaining four pairs [$6A\beta_{9-40}$, $5A\beta_{17-42}$], [$6A\beta_{9-40}$, $A\beta_{1-42}$], [$A\beta_{1-40}$, $5A\beta_{17-42}$] and [$A\beta_{1-40}$, $A\beta_{1-42}$], the correlation level is $R = 0.80$, 0.94, 0.74 and 0.92, respectively (Figure S4). Thus, E_{bind} obtained for $A\beta_{1-42}$ shows the highest correlation with $6A\beta_{9-40}$ ($R = 0.94$) but not with $5A\beta_{17-42}$.

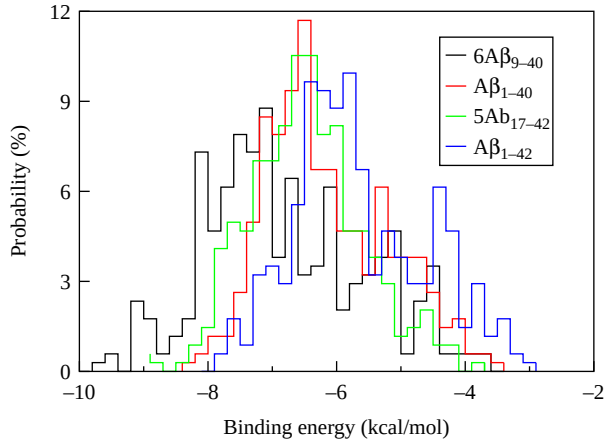

Figure 1. (Colour online) Distributions of binding energies of 342 ligands to four receptors. Results were obtained for best modes of docking using the Autodock Vina version 1.1 [19]. The energy bin used for obtaining these distributions is 0.2 kcal/mol. The average values of E_{bind} are -6.6, -5.9, -6.2 and -5.5 kcal/mol for $6A\beta_{9-40}$ (black), $A\beta_{1-40}$ (red), $5A\beta_{17-42}$ (green) and $A\beta_{1-42}$ (blue), respectively.

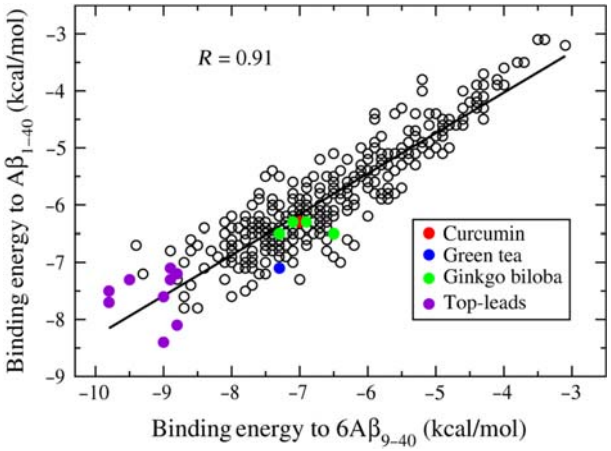

Figure 2. (Colour online) Relationship between binding energies to $A\beta_{1-40}$ and $6A\beta_{9-40}$. The correlation level $R = 0.91$. Violet, red, blue and green refer to top-leads, curcumin, green tea and gingko biloba, respectively.

Overall, the correlation between four sets of E_{bind} is high but this does not mean they provide exactly the same binding affinity ranking. Solasodine and Diosgenin show the highest susceptibility to $6A\beta_{9-40}$ with $E_{bind} = -9.8$ kcal/cal (Table S1 in SI), whereas Kulolactone has the lowest binding energy $E_{bind} = -8.9$ kcal/cal to $5A\beta_{17-42}$ (Table S2). If we make ranking by binding energies to $A\beta_{1-40}$, then Dracorubin occupies the first place having $E_{bind} = -8.4$ kcal/cal (Table S3 in SI). Sorting ligands by E_{bind} to monomer $A\beta_{1-42}$, Amentoflavone occupies the first place with $E_{bind} = -8.1$ kcal/cal (Table S4). It should be noted that binding energies are not correlated with either log(BB) or HIA (Figure S5 in SI).

3.3.2 *Top-leads revealed by docking results*

Since we have computed binding energies to four different receptors, there are several possibilities to screen out the best candidates to treat AD. These possibilities are discussed below.

Top-leads by ranking binding energies to $6A\beta_{9-40}$. In search for ligands that can degrade already formed fibrils of $A\beta_{9-40}$, we have to use E_{bind} obtained for this receptor. Among 342 compounds, we can choose 21 ligands with lowest binding energies from -9.8 to -8.5 kcal/mol (Table S1). However, Thevetine at position 17 should be

excluded not only because it has too low value of HIA (6%) but also low ability to cross the BBB ($\log(BB) = -1.57$). For the latter reason, Lactucopicrin (position 15) should also be disregarded. Dracorubin

Solasodine, Diosgenin, *Hinokiflavone*, Kulactone, Sarsasapogenin, *Dracorubin*, *Taraxasterol*, *Hecogenin*, Tanshinone, Kulolactone, Sanguinarine, *Taraxerol*, *Amentoflavone*, Limonin, Cycloartenol, TanshinonII, Melianodiol, Peiminine, Melianol.

(position 6) has relatively low value of $\log(BB) = -1.25$ but this value is still acceptable if one compares it with other existing drugs [35]. Therefore, for degradation of $A\beta_{1-40}$ aggregates, we recommend the following 19 top-hit compounds:

Curcumin (diferulom-rthane), ginkgo biloba (Ginkgolides A, B, C and J) and EGCG from the traditional Chinese and Indian medicines have E_{bind} higher than -7.3 kcal/mol and their ranking among 342 compounds is lower than 119 (Table S1). Thus, based on the virtual screening results, new top 19-leads are more promising than these compounds in treatment of AD.

Twenty-three top-leads sorted by binding energies to $5A\beta_{17-42}$. Table S2 in SI shows 27 ligands with lowest binding energies to this receptor ($-8.9 \le E_{bind} \le -7.5$ kcal/mol). These ligands are supposed to slow down the $A\beta_{1-42}$ fibril formation better than other compounds. As

Dracorubin, *Amentoflavone*, Peiminine, Diosgenin, *Taraxasterol*, Rottlerin, Limonin, *Solasodine*, Tetrandrine, Peimine, *Hinokiflavone*, *Hecogenin*, Sanguinarine, Arnidiol, *Taraxerol*, Glochidonol, Sarsasapogenin, Liriodenine

in the case of $6A\beta_{9-40}$, Scillaren A (position 9), Liquiritin (position 11) and Piperine (position 19) in Table S2 should be excluded due to their low ability to cross the BBB. Gomphrenin (position 18) is also skipped having HIA = 11%. Thus, we have the following 23 top-leads:

Comparing two sets of top-leads in Boxes (7) and (8), we can see that they share 11 common compounds (Solasodine, Hinokiflavone, Kulactone, Dracorubin, Taraxasterol, Tanshinone, Sanguinarine, Taraxerol, Amentoflavone, Cycloartenol and Hecogenin) which may slow down or prevent the fibril growth of both β_{1-40} and β_{1-42} peptides.

Eighteen top-leads by ranking binding energies to monomer $A\beta_{1-40}$. On Table S3 in SI (online only), we list 21 ligands that have lowest binding energies to this target ($-8.4 \le E_{bind} \le -7.2$ kcal/mol). They are

Kulolactone, *Dracorubin*, Bixin, Kulactone, Lobeline, *Hinokiflavone*, Adynerin, *Taraxerol*, Crocetin, Mangostin, Glycosminine, *Hecogenin*, Cycloartenol, Tanshinone, Cyclolaudenol, *Amentoflavone*, *Taraxasterol*, *Solasodine*, Sanguinarine, Conessine, Cannabinol, Arborine, Kaempferide.

expected to display high propensity to prevent $A\beta_{1-40}$ peptides from aggregation. Excluding Lactucopicrin (position 3), Thevetine (position 11) and Gomphnerin I (position 16) as having low HIA and log(BB), we obtain the following 18 top-leads:

From Boxes (7)–(9), it follows that three sets of top-leads share eight common ligands: Solasodine, Hinokiflavone, Dracorubin, Taraxasterol, Sanguinarine, Taraxerol, Hecogenin and Amentoflavone.

Eighteen top-leads sorted by binding energies to monomer $A\beta_{1-42}$. As evident from Table S4 in SI, 23 ligands have lowest binding energies in the interval $-8.1 \le E_{bind} \le -7.0$ kcal/mol. After exclusion of Corilagin (position 5), Tomatin (position 8), Tiliroside (position 12), Thevetine (position 15) and Lactucopicrin (position 20) which possess low HIA and log(BB), we have the following 18 top-leads:

Amentoflavone, *Hinokiflavone*, *Solasodine*, Diosgenin, *Hecogenin*, Sarsasapogenin, Tigogenin, *Dracorubin*, *Taraxerol*, Kulolactone, Adynerin, Arnidiol, Kulactone, *Taraxasterol*, Glochidonol, Chlorogenin, RhodexinA, Glochidiol.

Comparing this set with eight common ligands obtained for previous three sets, one can show that they share seven common ligands which are the best for all four energy sets. They are *Solasodine, Hinokiflavone, Dracorubin, Taraxasterol, Taraxerol, Hecogenin and Amentoflavone*.

Universal top-leads by ranking binding energies of all four sets. Seven ligands given in italics in Boxes (7)–(10) are qualified as universal top-leads by ranking of four energy sets. They are also able to cross the BBB as well as be absorbed by the human body. Because these ligands can bind well to all four receptors $6A\beta_{9-40}$, $5A\beta_{17-42}$, $A\beta_{1-40}$ and $A\beta_{1-42}$, they are supposed to interfere with oligomerisation and to degrade mature fibrils of amyloid peptides. Note that the list of seven common top-leads does not involve Diosgenin (champion of the first set in

Table 1. Nine top-leads revealed by ranking binding energies.

No.	ID	Herbs name	Compound	$6A\beta_{9-40}$	$A\beta_{1-40}$	$5A\beta_{17-42}$	$A\beta_{1-42}$	Log(BB)	HIA (%)
1	31342	*S. xanthocarpum* Schrad	Solasodine	−9.8	−7.5	−7.5	−7.6	0.84	94
2	99474	*Schizocapsa plantaginea* Hance	Diosgenin	−9.8	−7.7	−7.4	−7.5	0.89	96
3	5281627	*T. orientalis* L.	Hinokiflavone	−9.5	−7.3	−8.0	−7.6	−0.94	87
4	160270	*C. draco* Willd	Dracorubin	−9.0	−8.4	−8.7	−7.3	−1.25	98
5	5270604	*Centipeda minima*	Taraxasterol	−9.0	−7.6	−7.5	−7.0	1.36	100
6	5318868	*Melia azedarach* L.	Kulolactone	−8.9	−7.1	−8.9	−7.1	1.03	96
7	91453	*Agave americana* Lin.	Hecogenin	−8.9	−7.3	−7.6	−7.4	0.26	96
8	92097	*T. officinale*	Taraxerol	−8.8	−7.2	−7.9	−7.2	1.32	100
9	5281600	*Selaginella tamariscina*	Amentoflavone	−8.8	−8.1	−7.5	−8.1	−0.93	81

Notes: They include seven common ligands given in italics in Boxes (7)–(10), Diosgenin from Table S1 and Kulolactone from Table S2 (in SI, online only). Second column refers to ID of ligands according to the Pubchem and Chemspider database. Binding energies are measured in kcal/mol.

Table S1), Kulolactone (champion of the second set in Table S2). We add these two ligands to the list of universal top-leads. Therefore, the full list of top-hits includes nine ligands and is shown in Table 1, in which the names of corresponding plants are also presented. Solasodine, for instance, comes from *Solanum xanthocarpum* Schrad, whereas Hinokiflavone, Dracorubin and Taraxerol are derived from *Thuja orientalis* L., *Calamus draco* Willd and *Taraxacum officinale*, respectively. Chemical structures of top-leads revealed by the docking method are shown in Figure 3.

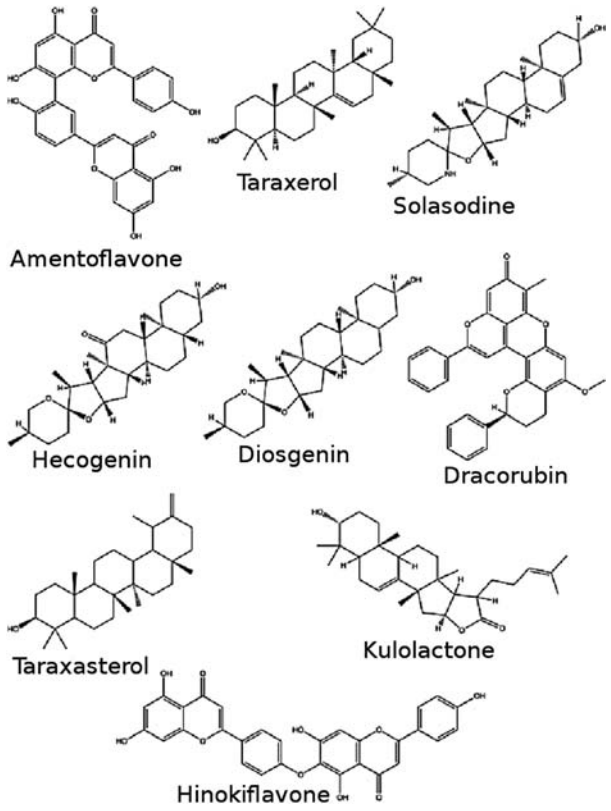

Figure 3. Chemical structures of nine top-leads revealed by the docking method. Their IDs are also shown.

In terms of binding energies, nine top-hit compounds (Table 1) are better than existing candidates Curcumin, ginkgo biloba and EGCG from green tea in preventing AD. However, the docking approach is not always accurate as it has a number of drawbacks related to omission of receptor dynamics and a limited number of trial positions of ligand. From this prospect, our conclusion that nine top-leads are superior to other intensively studied natural compounds should be re-examined by more sophisticated approaches. Below, this problem is considered using the MM-PBSA method.

3.3.3 *Hydrogen networks*

In this section, we focus on the nature of ligand binding to different receptors in the framework of the docking approach. For illustration, we consider ligands Solasodine, Dracorubin, Kulolactone, Amentoflavone and Hinokiflavone from nine top-leads (Table 1). The best position of Solasodine in the $6A\beta_{9-40}$ fibril is shown in Figure 4(A). It is in the turn region of upper peptides B, D and F. Although there exists only one HB between the ligand and Lys28 of the receptor (Figure 4(B)), the corresponding energy remains high ($E_{bind} = -9.8$ kcal/mol). Since HB energy is 1–5 kcal/mol, other interactions like the Coulomb and vdW interactions also contribute to E_{bind} of Solasodine.

Dracorubin, positioned near the N-terminal of $A\beta_{1-40}$ (Figure 4(C)), shows the highest binding affinity to this monomer with $E_{bind} = -8.4$ kcal/mol (Table 1). It also forms only one HB with Gly9 of the target (Figure 4(D)) implying that other contributions are important in complex association. Dracorubin strongly binds to both mature fibrils (see the binding energies on Table 1), whereas its coupling with $A\beta_{1-42}$ is relatively weak.

Among 342 ligands, Kulolactone displays the highest binding affinity to protofibril $5A\beta_{17-42}$ with $E_{bind} = -8.9$ kcal/mol. In the best docking mode, it locates next to peptide A of the receptor (Figure 5(A)) but no HB is formed. Thus, the binding of this ligand is entirely defined by the Coulomb and vdW interactions.

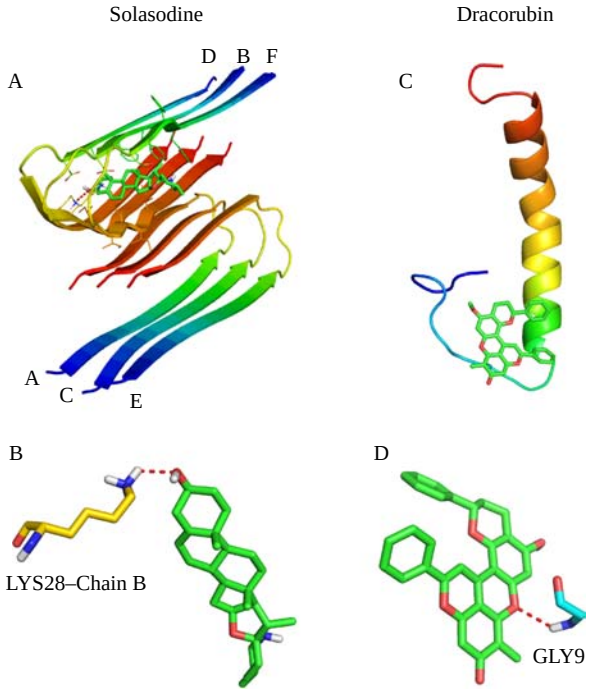

Figure 4. (Colour online) The best binding position of Solasodine to $6A\beta_{9-40}$ (A) and the corresponding HB network (B). (C) and (D) are the same as in (A) and (B) but for Dracorubin-$A\beta_{1-40}$ complex. In both cases, only one HB occurs between ligand and target.

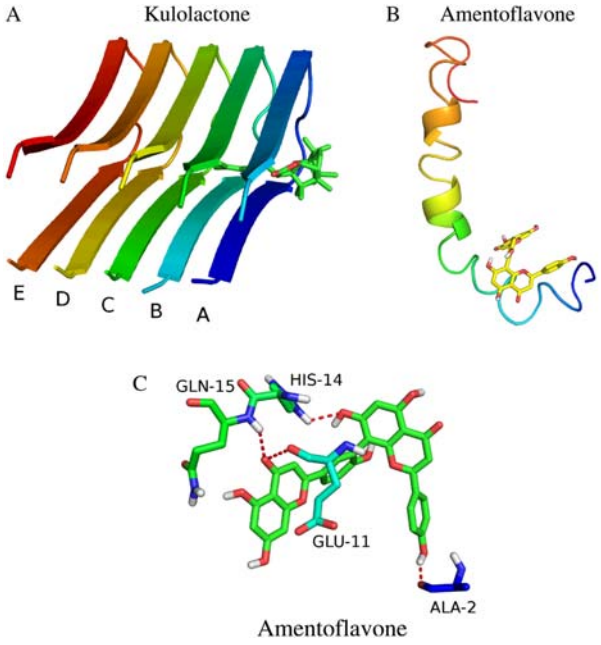

Figure 5. (Colour online) (A) The binding place of Kulolactone to fibril $5A\beta_{17-42}$. There is no HB between these two compounds. (B) The docking position of Amentoflavone to monomer $A\beta_{1-42}$ and the corresponding HB network (C). There are four HBs between the ligand and the receptor.

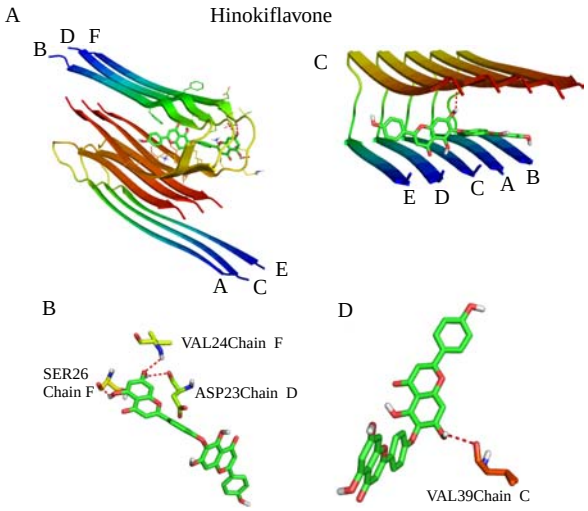

Figure 6. (Colour online) The binding place of Hinokiflavone to the fibril $6A\beta_{9-40}$ (A) and the corresponding HB network (B). HB is formed with Ser26, Val24 and Asp23 from chains F and D of fibril. (C) and (D) are the same as in (A) and (B) but for docking of Hinokiflavone to $5A\beta_{17-42}$. There is only one HB between ligand and Val39 of chain C of $5A\beta_{17-42}$.

HB plays an important role in association of Amentoflavone with monomer $A\beta_{1-42}$ near the N-terminal (Figure 5(B)) because four HBs occur between the ligand and amino acids Ala2, Glu11, His 14 and Gln15 of the target. It has the same binding energy $E_{\text{bind}} = -8.1$ kcal/mol to both monomers $A\beta_{1-42}$ and $A\beta_{1-40}$, but one has only three HBs with the latter (results not shown).

To illustrate diversity of HB to different receptors, we consider Hinokiflavone as an example. Similar to Solasodine, this compound is bound to $6A\beta_{9-40}$ in the turn region inside fibril (Figure 6(A)). The difference is that Hinokiflavone has three HBs with $6A\beta_{9-40}$ (Figure 6(B)), whereas Solasodine has only one HB (Figure 4(B)). This may be associated with the fact that the former has 10 HB acceptors and 5 HB donors, whereas the latter has 3 HB acceptors and 2 HB donors. Contrary to $6A\beta_{9-40}$, Hinokiflavone locates at the end of peptides of $5A\beta_{17-42}$ (Figure 6(C)), having one HB with Val39 of chain C (Figure 6(D)). In the best docking mode, this compound locates near the N-terminal of monomers $A\beta_{1-40}$ and $A\beta_{1-42}$ (Figure S6 in SI, online only). It forms two HBs with Asp1 and Gln15 of the former and one HB with Glu11 of the latter (Figure S6).

In short, our analysis reveals that in some cases, for instance binding of Amentoflavone to $5A\beta_{17-42}$, HB plays an important role. However, for many complexes ($6A\beta_{9-40}$–Kulolactone, $5A\beta_{17-42}$–Taraxerol, $6A\beta_{9-42}$–Taraxerol, etc.), this type of bonding is irrelevant. Such a situation occurs when the number of HB donors and acceptors of ligands is small (Taraxerol has only one HB donor and one HB acceptor). In this case the electrostatic and vdW interactions become dominating.

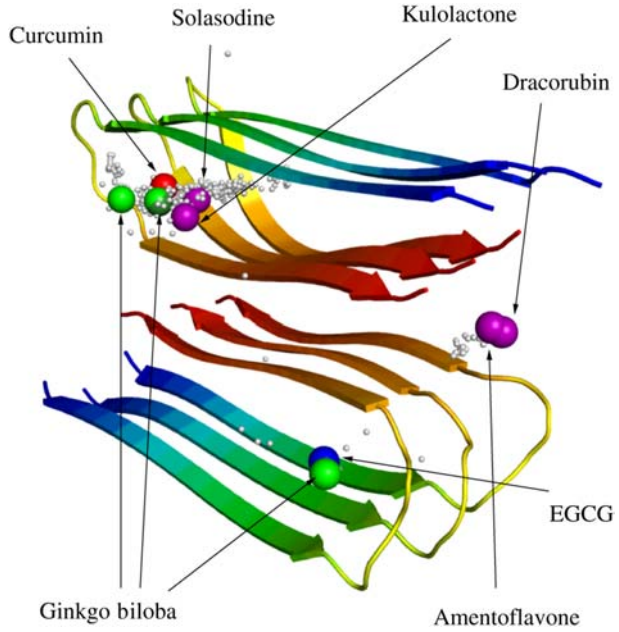

Figure 7. (Colour online) Binding positions of different ligands (Curcumin, gingko biloba including Ginkgolides A, B, C and J, EGCG, Solasodine, Kulolactone, Dracorubin and Amentoflavone) around fibril $6A\beta_{9-40}$.

3.3.4 Diversity of locations of ligands in the best docking mode

Docking positions of representative ligands to receptor $6A\beta_{9-40}$ are shown in Figure 7. Clearly, they vary from ligand to ligand. Amentoflavone and Dracorubin from nine top-leads locate between two layers, whereas, similar to Curcumin, EGCG and ginkgo biloba, Solasodine and Kulolactone are inside one layer. In the case of $5A\beta_{17-42}$ Solasodine, Dracorubin and EGCG prefer to be outside of the fibril, whereas other compounds stay inside (Figure 8).

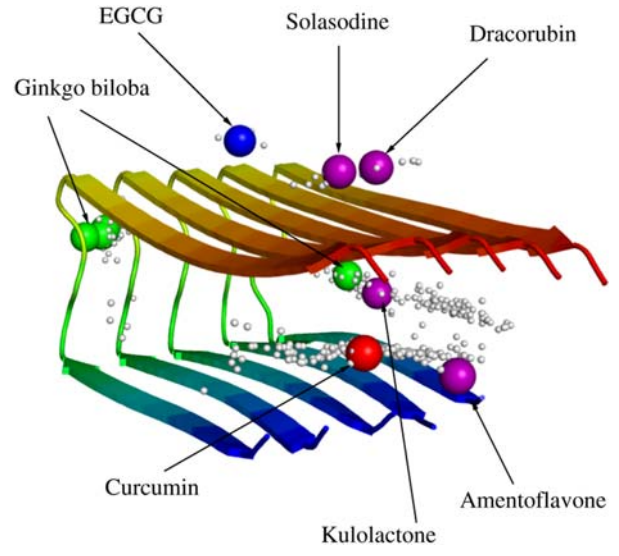

Figure 8. (Colour online) The same as in Figure 7 but for $5A\beta_{17-42}$.

Thus, only Dracorubin favours to be outside of the layer in both cases. As evident from Figure S7 in SI, all of the considered ligands are located near the N-terminal of monomer $A\beta_{1-40}$. The situation becomes very different in the $A\beta_{1-42}$ case, in which Curcumin, Amentoflavone, EGCG and one of ginkgo biloba ligands are positioned at the N-end, whereas Kulolactone prefers to be in the middle (Figure S8 in SI). Other molecules are energetically more favourable to locate at the C-termini.

3.4 Refinement of docking results by the MM-PBSA method

Since the docking method is not accurate enough for prediction, we refine our finding by calculating the binding free energy of nine top-leads using a more reliable MM-PBSA method (Section 2). Because docking results obtained for different targets show high correlation, only $6A\beta_{9-40}$ was chosen as a receptor for MD simulations.

For each system, we had carried out MD run of 19ns except that MD run of 29 ns simulation was carried out for compound Solasodine. Since all systems behave in a similar way, we show results for four ligands Dracorubin, Hinokiflavone, Kulolactone and Hecogenin that have very different binding free energies (see Table 2). From the time dependence of backbone RMSD from the initial structures (Figure 9), it is clear that these systems get equilibrium at different time t_{eq} ($t_{eq} \approx 13$, 9, 13 and 11 ns for Dracorubin, Hinokiflavone, Kulolactone and Hecogenin, respectively). Snapshots collected every 10 ps after t_{eq} were used for calculating ΔG_{bind} by the MM-PBSA method (Section 2) and the results are shown in Table 2. The entropic ($T\Delta S$) and non-polar contribution (ΔG_{sur}) are not sensitive to ligands. For all systems, the vdW interaction dominates over the electrostatic interaction (Figure S9 in SI). The low binding affinity of Kulolactone is mainly associated with repulsion between the receptor and ligand.

In order to understand the nature of ligand binding, we have monitored the time dependence of the number of HBs between the ligand and the receptor (Figure 10) and calculated its average value in the equilibrium. Ligand Dracorubin has higher binding affinity than Hinokiflavone but its HB network is weaker (Figure 10) because the average number of HBs of the former is equal to 0.33 whereas that of Hinokiflavone is 1.03. In equilibrium Hecogenin and Kulolactone have almost the same average number of HBs (≈ 0.1) but they show different resistance to $6A\beta_{9-40}$, suggesting that HBs alone do not govern the binding affinity. Using results shown in Figure 11, we obtain the equilibrium average number of SC contacts between receptor and the ligand equal 5.83, 2.87, 2.28 and 1.04 for Dracorubin, Hinokiflavone, Hecogenin and Kulolactone, respectively. Thus, the higher is the binding affinity (Table 2) the stronger is the SC interaction. The dominance of SC contacts is also illustrated in Figure S10, in which the

Table 2. Binding free energies (in units of kcal/mol) to $6A\beta_{9-40}$ of nine top-leads revealed by the docking method.

No.	ID	Ligand	$-T\Delta S$	ΔE_{vdW}	ΔE_{elec}	ΔG_{PB}	ΔG_{sur}	ΔG_{bind}
1	160270	Dracorubin	21.22	−58.36	−12.06	37.73	−4.12	−15.59
2	92097	Taraxerol	19.04	−41.73	−1.07	12.76	−3.85	−14.85
3	5270604	Taraxasterol	20.25	−50.88	0.03	22.42	−3.95	−12.13
4	5281627	Hinokiflavone	24.16	−55.69	−18.34	42.41	−4.39	−11.85
5	99474	Diosgenin	20.36	−52.25	−4.35	29.61	−4.47	−11.1
6	91453	Hecogenin	19.69	−50.32	−3.07	31.77	−4.21	−6.14
7	5281600	Amentoflavone	21.81	−43.57	0.26	19.88	−3.26	−4.88
8	31342	Solasodine	23.35	−38.60	−118.29	132.4	−3.23	−4.37
9	5318868	Kulolactone	22.68	−45.03	7.39	16.86	−4.30	−2.40

Note: Results were obtained by the MM-PBSA method.

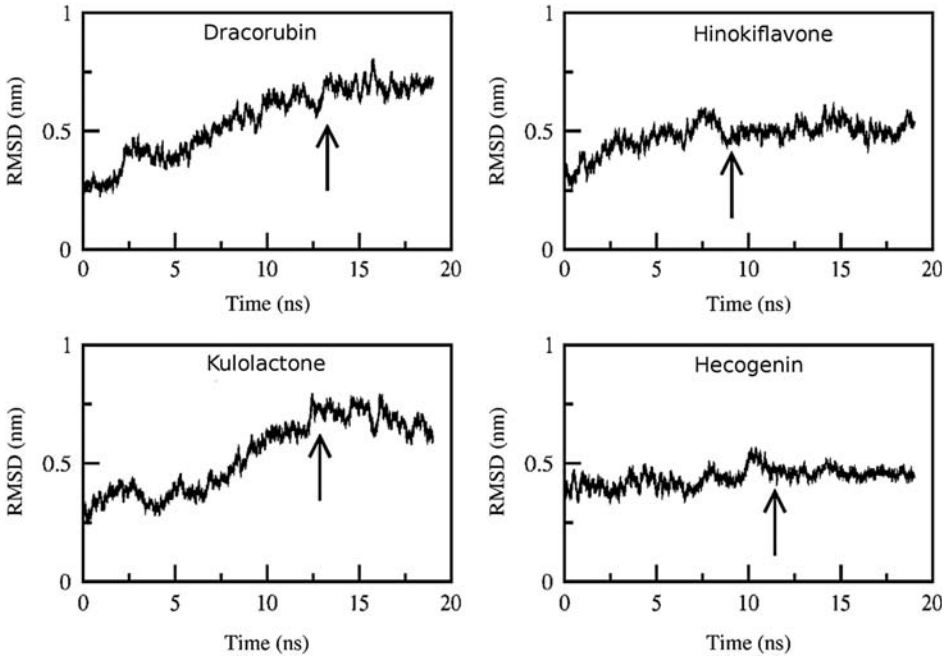

Figure 9. Time dependence of RMSD for four compounds. Arrow refers to equilibrium time t_{eq} when the system reaches equilibrium.

typical conformation of $6A\beta_{9-40}$–Hinokiflavone in equilibrium is shown. Here, Hinokiflavone has three HBs against five SC contacts (not shown) with the target.

The ranking of binding affinity obtained by the MM-PBSA method (Table 2) is very different from the ranking of docking as the correlation level between two sets of results is almost zero (Figure 11 in SI). Ligand 160270 ranked fourth by docking (Table 1) becomes a champion in MM-PBSA (Table 2). Since the latter method is more accurate, we should rely on its results. Keeping only ligands that have $\Delta G_{bind} < -11$ kcal/mol, we predict that Dracorubin, Taraxerol, Taraxasterol, Hinokiflavone and Diosgenin may be good candidates to cope AD. Using the relationship between the binding free energy and inhibition constant K_i ($\Delta G_{bind} = RT \ln(K_i)$, where the gas constant $R = 1.987 \times 10^{-3}$ kcal/mol), we can show that K_i of five top-leads varies between 8 nM and 4 pM. In other words, they have excellent inhibitory capacity. Having used the MM-PBSA and the same force field and water model, we have obtained the binding free energy of Curcumin to $6A\beta_{9-40}$ $\Delta G_{bind} \approx -14.3$ kcal/mol (Son Tung Ngo and Mai Suan Li, unpublished results). Using the experimental value $K_i = 0.2$ nM [54], we obtain $\Delta G_{bind} \approx -13.3$ kcal/mol for binding of Curcumin to $A\beta_{9-40}$ aggregates. Therefore, the binding affinity of Dracorubin and Taraxerol to the Aβ fibrils is probably compatible or even higher than Curcumin.

3.5 Comparison of pharmacological properties of top leads with Curcumin

Curcumin has HIA of 94% (Table S1) which is higher than that of Hinokiflavone (87%) but lower than that of four other top leads (Table 1). Thus, Taraxerol, Taraxasterol, Diosgenin and Dracorubin may be better absorbed by

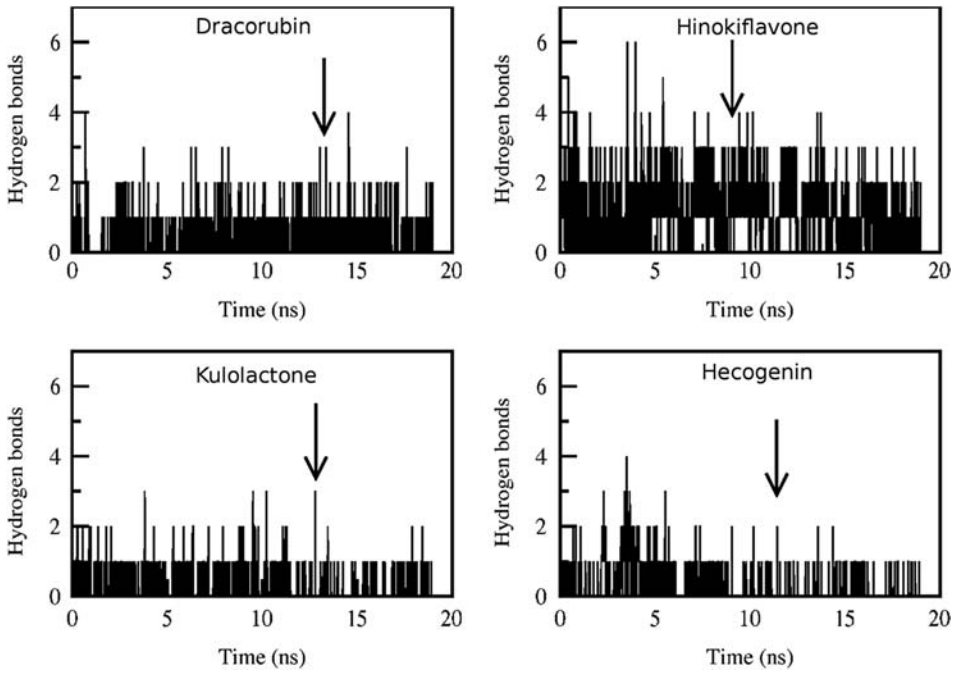

Figure 10. The same as in Figure 9 but for the number of HBs between the ligand and receptor. The average number of HBs in equilibrium is 0.33, 1.03, 0.10 and 0.11 for Dracorubin, Hinokiflavone, Hecogenin and Kulolactone, respectively.

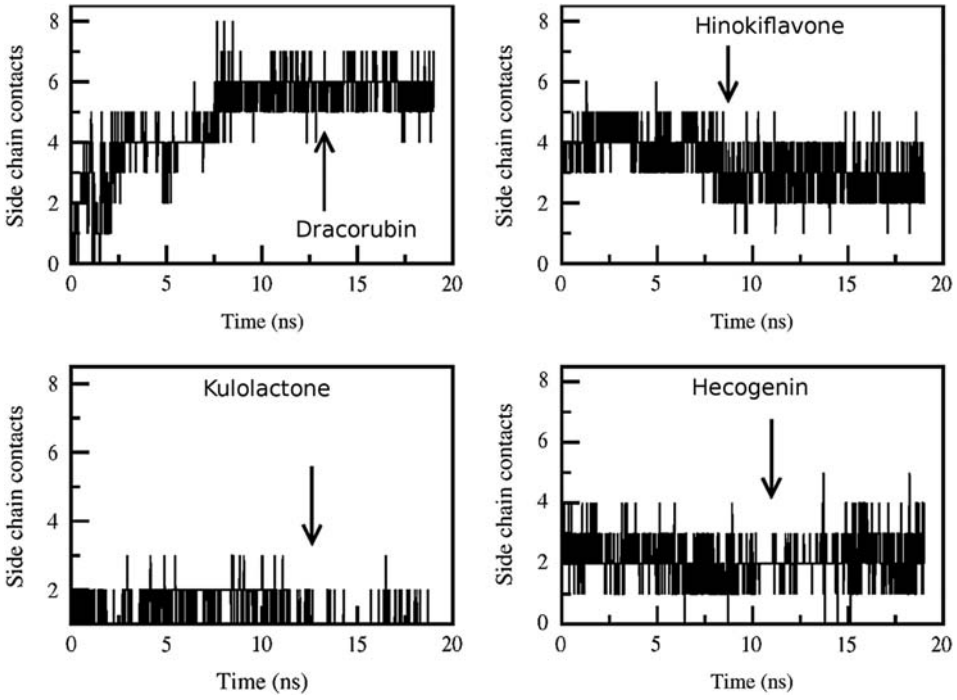

Figure 11. The same as in Figure 9 but for the number of contacts between SCs of receptor and ligand. The average number of these contacts in equilibrium is 5.83, 2.87, 2.28 and 1.04 for Dracorubin, Hinokiflavone, Hecogenin and Kulolactone, respectively.

human body than Curcumin, but all of these compounds have high HIA (>85%). Taraxerol, Taraxasterol, Diosgenin and Hinokiflavone are supposed to cross the BBB better than Curcumin which has log(BB) = −1.04 (Tables 1 and S1). Having log(BB) = −1.25, Dracorubin is presumably worse than Curcumin in jumping over BBB.

With the help of PreADME server, we have analysed the toxicity of five top-leads and Curcumin (Table S5 in SI).

Together with Curcumin, Taraxerol and Diosgenin pass the Ames test. The remaining three top compounds may act as a carcinogen (or cause cancer), being positive to this test. Since Taraxerol is positive to both rat and mouse carcinogenicity, it is probably more toxic than Diosgenin and Curcumin. Thus, in terms of toxicity, our analysis reveals that Diosgenin is likely compatible with Curcumin, whereas other top-leads are more toxic.

Using software QikProp v3.3 (http://www.schrodinger.com/products/14/17/), we have studied metabolism for five top-leads and Curcumin (see page 64 in SI). For Curcumin oxidation of two aromatic OH (the structure of Curcumin is available on position 155 of Table S1), alpha hydroxylation of carbonyl and ether dealkylation may take place. The aromatic OH oxidation is also possible for Hinokiflavone having five aromatic OH atoms (Figure 3) but not for other top-leads. Due to the existence of aromatic OH that can eliminate free radicals, Curcumin and Hinokiflavone are supposed to be not highly toxic. However, reactive functional groups (page 64 in SI) in Curcumin and Diosgenin may enhance their toxicity. Similar to that in Curcumin, the removal of alkyl group from ether likely takes place in Dracorubin. The conversion of benzylic-like H to alcohol can occur only in this compound. A secondary alcohol may be oxidised converting to a ketone in Taraxerol, Diosgenin and Taraxasterol. Alcohol can also be produced from allylic H in these three ligands.

Overall, metabolism pathways are similar for Taraxerol and Diosgenin, whereas Curcumin shares some pathways with Hinokiflavone and Dracorubin. However, we have to bear in mind that theoretical predictions may be false, and further biochemical and pharmacore studies are vital to settle this problem.

3.6 Competition between fibril growth and ligand binding

Since fibril elongation and ligand binding may occur concurrently, it is worth to study the competition between these two processes. For this purpose, we use the protein docking method [55–58] implemented in the ClusPro software (http://cluspro.bu.edu/login.php) to dock full-length and truncated Aβ peptides to fibrils $5A\beta_{17-42}$ and $6A\beta_{9-40}$. Because the results are quite similar for two targets, we focus on the first target. Structure of $A\beta_{42}$ is taken from PDB (PDB ID: 1Z0Q), whereas the structure of $A\beta_{17-42}$ is extracted from fibril $5A\beta_{17-42}$ (PDB ID: 2BEG). The position of $A\beta_{42}$ and $A\beta_{17-42}$ in the best docking mode to $5A\beta_{17-42}$ is shown in Figure 12, where five top-leads and Curcumin are also presented. The binding of $A\beta_{17-42}$ is more tight than that of $A\beta_{42}$ with the binding energy equal to −318.5 and −204.3 kcal/mol, respectively. $A\beta_{17-42}$ forms 56 SC contacts with $5A\beta_{17-42}$, whereas $A\beta_{42}$ has only nine SC contacts.

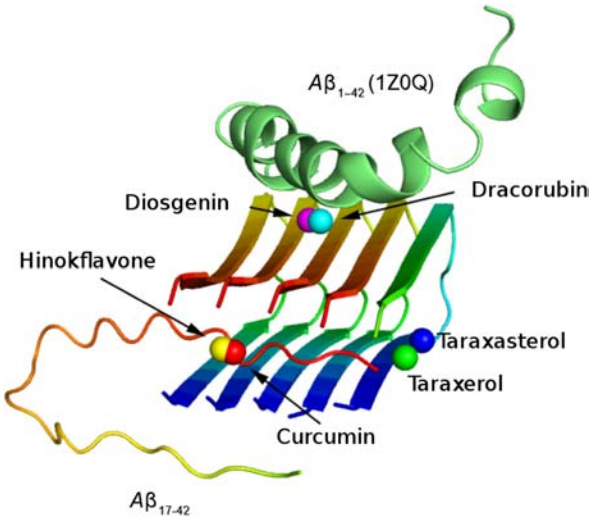

Figure 12. (Colour online) Positions of $A\beta_{42}$ (green) and $A\beta_{17-42}$ (red and yellow) in the best docking mode to $5A\beta_{17-42}$. The binding energy is equal to −204.3 and −318.5 kcal/mol for $A\beta_{42}$ and $A\beta_{17-42}$, respectively. The result was obtained by the protein–protein docking method. Circles refer to centres of mass of five top-leads and Curcumin in the best docking positions.

Since there are no HBs between the target and two peptides, the binding affinity is controlled by SC contacts.

Obviously, $A\beta_{42}$ can interfere with binding of Dracorubin and Diosgenin (Figure 12) as they are close to each other. The truncated peptide $A\beta_{17-42}$ has the docking position different from that of $A\beta_{42}$ and may interact with Curcumin and Hinokiflavone modulating their binding dynamics. Taraxerol and Taraxasterol do not have contacts with either $A\beta_{42}$ or $A\beta_{17-42}$ in the best docking mode but they may strongly interfere with aggregation because the fibril growth is expected to occur on the fibril edge. Interestingly, in the third docking mode with the binding energy of −309.2 kcal/mol, of the position $A\beta_{17-42}$ is almost commensurable with the fibril lattice (Figure S12). In this position, the docked peptide has a strong interaction with Taraxerol and Taraxasterol.

Thus, the fibril growth may compete with ligand binding. But this scenario follows from the docking simulation and it may change should the real dynamics be taken into account.

4. Conclusion

For the first time, we have carried out the systematic computational study of 342 ligands derived from plants and herbs as potential leads to treat AD. Our main results and further remarks are as follows:

(1) We have shown that most of the compounds can be absorbed by the human body, pass through the BBB and have high binding energies to $6A\beta_{9-40}$, $A\beta_{1-40}$, $5A\beta_{17-42}$ and $A\beta_{1-42}$.
(2) The role of HB in binding of ligands to four receptors

is studied in detail using the docking method. In most of the cases together with HBs, the electrostatic and vdW interactions make important contribution to E_{bind}. For some complexes, the HB is minor and this conclusion is also confirmed by the MM-PBSA method.

(3) Locations of ligands in the best docking mode depend not only on ligands themselves but also on receptors (Figures 7, 8 and S6–S8).

(4) With the help of the docking and MD simulations, we predict that there are five top-leads (Table 2) that may not only slow down aggregation but also degrade mature fibrils of amyloid peptides. Two of them (Dracorubin and Taraxerol) are more prominent than Curcumin for treating AD which have lower ΔG_{bind}. Five top-leads are derived from plants shown in Figure S13 of SI.

(5) Pharmacological characteristics such as HIA, BBB, toxicity and metabolism have been analysed for top-leads and Curcumin. But our theoretical predictions are just consultative and have to be carefully verified by *in vivo* experiments.

(6) We have considered all of the 342 compounds with known chemical structures from the book of Loi [18]. We believe that more ligands derived from Vietnamese herbs and plants should be available but scattered in different sources. Our next task is to collect them and update our results.

Supporting Information: Table S1 shows E_{bind}, log(BB) and HIA for all 342 ligands, whereas Tables S2–S4 represent top-hit compounds according to binding energies obtained for receptor $5A\beta_{17-42}$, $A\beta_{1-40}$ and $A\beta_{1-42}$. Additional figures describe correlation between binding energies from different sets, the relationship between E_{bind}, log(BB) and HIA, hydrogen networks, positions of ligands around receptors as well as the time dependence of vdW and electrostatic interaction energies. This material is available free of charge via the Internet at http://www.tandfonline.com.

Acknowledgements

This work was supported by Narodowe Centrum Nauki in Poland (Grant No. 2011/01/B/NZ1/01622) and the Department of Science and Technology at Ho Chi Minh City, Vietnam. We thank N.T.N. Tam for very useful discussions on metabolism. Allocation of CPU time at the supercomputer center TASK in Gdansk (Poland) is highly appreciated.

References

[1] J. Hardy and D.J. Selkoe, *The amyloid hypothesis of Alzheimer's disease: Progress and problems on the road to therapeutics*, Science 297 (2002), pp. 353–356.

[2] L.O. Tjerngber, J. Naslund, F. Lindqvist, J. Jahannson, A.R. Karlstrom, J. Thyberg, L. Terenius, and C. Nordstedt, *Arrest of beta-amyloid beta-peptide fibril formation by a pentapeptide*, J. Biol. Chem. 271 (1996), pp. 8545–8548.

[3] C.M. Soto, S. Kindy, M. Baumann, and B. Frangione, *Inhibition of Alzheimer's amyloidosis by peptides that prevent β-sheet conformation*, Biochem. Biophys. Res. Commun. 226 (1996), pp. 672–680.

[4] C. Adessi and C. Soto, *Beta-sheet breaker strategy for the treatment of Alzheimer's disease*, Drug Dev. Res. 56 (2002), pp. 184–193.

[5] H.Y. Li, M.B. Monien, A. Lomakin, R. Zemel, E.A. Fradinger, M.A. Tan, S.M. Spring, B. Urbanc, C.W. Xie, G.B. Benedek, and G. Bitan, *Mechanistic investigation of the inhibition of A beta 42 assembly and neurotoxicity by A beta 42 C-terminal*, Biochemistry 49 (2010), pp. 6358–6364.

[6] C. Wu, M.M. Murray, S.L.B.L. Summer, M.M. Condron, G. Bitan, J.E. Shea, and M.T. Bowers, *The structure of A beta 42 C-terminal fragments probed by a combined experimental and theoretical study*, J. Mol. Biol. 387 (2009), pp. 492–501.

[7] D.J. Gordon, R. Tappe, and S.C. Meredith, *Design and characterization of a membrane permeable N-methyl amino acid-containing peptide that inhibits A beta(1-40) fibrillogenesis*, J. Pept. Res. 60 (2002), pp. 37–55.

[8] R.E.W. Christopher, M. Ranger, A.P. Singh, M.E. Reding, J.M. Frantz, J.C. Locke, and C.R. Krause, *Rare excitatory amino acid from flowers of zonal geranium responsible for paralyzing the Japanese beetle*, Proc. Natl. Acad. Sci. USA 108 (2011), pp. 1217–1221.

[9] C.A. Hawkes, V. Ng, and J. MacLaurin, *Small molecue inhibitors of Aβ-aggregation and neurotoxity*, Drug Dev. Res. 70 (2009), pp. 111–124.

[10] G. Yamin, K. Ono, M. Inayathullah, and D.B. Teplow, *Amyloid β-protein assembly as therapeutic target of Alzheimer's disease*, Curr. Pharm. Des. 14 (2008), pp. 3231–3246.

[11] P. Williams, A. Sorribas, and M.J.R. Howes, *Natural products as a source of Alzheimer's drug leads*, Nat. Prod. Rep. 28 (2011), pp. 48–77.

[12] M.J.R. Howes and P.J. Houghton, *Plants used in Chinese and Indian traditional medicine for improvement of memory and cognitive function*, Pharmacol. Biochem. Behav. 75 (2003), pp. 513–527.

[13] F.S. Yang, G.P. Lim, A.N. Begum, O.J. Ubeda, M.R. Simmons, S.S. Ambegaokar, P.P. Chen, R. Kayed, C.G. Glabe, S.A. Frautschy, and G.M. Cole, *Curcumin inhibits formation of amyloid beta oligomers and fibrils, binds plaques, and reduces amyloid* in vivo, J. Biol. Chem. 280 (2005), pp. 5892–5901.

[14] Y. Luo, J.V. Smith, V. Paramasivam, A. Burdick, K.J. Curry, J.P. Buford, L. Khan, W.J. Netzer, H.X. Xu, and P. Butko, *Inhibition of amyloid-beta aggregation and caspase-3 activation by the Ginkgo biloba extract EGb761*, Proc. Natl. Acad. Sci. USA 99 (2002), pp. 12197–12202.

[15] S. Bastianetto, Z.X. Yao, V. Papadopoulos, and R. Quirion, *Neuroprotective effects of green and black teas and their catechin gallate esters against beta-amyloid-induced toxicity*, Eur. J. Neurosci. 23 (2006), pp. 55–64.

[16] J.M. Ringman, S.A. Frautschy, G.M. Cole, D.L. Masterman, and J.L. Cummings, *A potential role of the curry spice curcumin in Alzheimer's disease*, Curr. Alzheimer Res. 2 (2005), pp. 131–136.

[17] S.T. DeKosky, *Ginkgo biloba prevention trial in order individuals*, (2010), National Center for Complementary and Alternative Medicine. Available at http://www.clinicaltrials.gov/ct2/show/NCT00010803.

[18] D.T. Loi, *Vietnam's Herbal Plants and Remedies ē (in Vietnamese)*, Medicine Publisher, Ha Noi, 2004.

[19] O. Trott and A.J. Olson, *Improving the speed and accuracy of docking with a new scoring function, efficient optimization, and multithreading*, J. Comput. Chem. 31 (2010), pp. 455–461.

[20] A.T. Petkova, Y. Ishii, J. Balbach, O. Antzutkin, R. Leapman, F. Delaglio, and R. Tycko, *A structural model for Alzheimer's beta-amyloid fibrils based on experimental constraints from solid state NMR*, Proc. Natl. Acad. Sci. USA 99 (2002), pp. 16742–16747.

[21] A.T. Petkova, W.M. Yau, and R. Tycko, *Experimental constraints on quaternary structure in Alzheimer's β-amyloid fibrils*, Biochemistry 45 (2006), pp. 498–512.

[22] T. Luhrs, C. Ritter, M. Adrian, D. Riek-Loher, B. Bohrmann, H. Doeli, D. Schubert, and R. Riek, *3D structure of Alzheimer's amyloid-beta(1-42) fibrils*, Proc. Natl. Acad. Sci. USA 102 (2005), pp. 17342–17347.

[23] M.D. Wessel, P.C. Jurs, J.W. Tolan, and S.M. Muskal, *Prediction of human intestinal absorption of drug compounds from molecular structure*, J. Chem. Inf. Comput. Sci. 38 (1998), pp. 726–735.

[24] S.K. Lee, I.H. Lee, H.J. Kim, G.S. Chang, J.E. Chung, and K.T. No, *The PreADME approach: Web-based program for rapid prediction of physico-chemical, drug absorption and drug-like properties*, *EuroQSAR 2002 Designing Drugs and Crop Protectants: Processes, Problems and Solutions*, Blackwell Publishing, Maldenh, MA, 2003, pp. 418–420.

[25] M. Coles, W. Bicknell, A.A. Watson, D.P. Fairlie, and D.J. Craik, *Solution structure of amyloid beta-peptide(1-40) in a water-micelle environment. Is the membrane-spanning domain where we think it is?* Biochemistry 37 (1998), pp. 11064–11077.

[26] S. Tomaselli, V. Esposito, P. Vangone, N.A. Nulandvan, A.M. Bonvin, R. Guerrini, T. Tancredi, P.A. Temussi, and D. Picone, *The alpha-to-beta conformational transition of Alzheimer's Abeta-(1-42) peptide in aqueous media is reversible: A step by step conformational analysis suggests the location of beta conformation seeding*, ChemBiochem 7 (2006), pp. 257–267.

[27] J.M. Wang, R.M. Wolf, J.W. Caldwell, P.A. Kollman, and D.A. Case, *Development and testing of a general amber force field*, J. Comput. Chem. 25 (2004), pp. 1157–1174.

[28] A. Jakalian, D.B. Jack, and C.I. Bayly, *Fast, efficient generation of high-quality atomic charges. AM1-BCC model: II. Parameterization and validation*, J. Comput. Chem. 23 (2002), pp. 1623–1641.

[29] M.F. Sanner, *Python: A programming language for software intergration and development*, J. Mol. Graph. Model 17 (1999), pp. 57–61.

[30] G.M. Morris, D.S. Godsell, R.S. Halliday, R. Huey, W.E. Hart, R.K. Belew, and A.J. Olson, *Automated docking using a Lamarckian genetic algorithm and an empirical binding free energy function*, J. Comput. Chem. 19 (1998), pp. 1639–1662.

[31] G.M. Morris, D.S. Goodsell, R. Huey, and A.J. Olson, *Distributed automated docking of flexible ligands to proteins: Parallel applications of AutoDock 2.4*, J. Comput. Aided Mol. Des. 10 (1996), pp. 293–304.

[32] D.F. Shanno, *Conditioning of quasi-Newton methods for function minimization*, Math. Comput. 24 (1970), pp. 647–656.

[33] P. Garg and J. Verma, *In silico prediction of blood brain barrier permeability: An artificial neural network model*, J. Chem. Inf. Model 46 (2006), pp. 289–297.

[34] P. Crivori, G. Cruciani, P. Carrupt, and B. Testa, *Predicting blood–brain barrier permeation from three-dimensional molecular structure*, J. Med. Chem. 43 (1998), pp. 2204–2216.

[35] K. Rose and L.H. Hal, *Modeling blood–brain barrier partitioning using the electrotopological state*, J. Chem. Inf. Comput. Sci. 42 (2002), pp. 651–666.

[36] D.E.R. Clark, *Calculation of polar molecular surface area and its application to the prediction of transport phenomena. 2. Prediction of blood–brain barrier penetration*, J. Pharm. Sci. 88 (1999), pp. 815–821.

[37] C.A. Lipinski, F. Lombardo, and B.W. Dominy, *Experimental and computational approaches to estimate solubility and permeability in drug discovery and development settings*, Adv. Drug Deliv. Rev. 23 (1997), pp. 3–25.

[38] Y.H. Zhao, J. Le, M.H. Abraham, A. Hersey, P.J. Eddershaw, C.N. Luscombe, D. Boutina, G. Beck, B. Sherborne, I. Cooper, and J.A. Platts, *Evaluation of human intestinal absorption data and subsequent derivation of a quantitative structure–activity relationship (QSAR) with the Abraham descriptors*, J. Pharm. Sci. 90 (2001), pp. 749–784.

[39] O.A. Raevsky, K.J. Schaper, P. Artursson, and J.W. McFarland, *A novel approach for prediction of intestinal absorption of drugs in humans based on hydrogen bond descriptors and structural similarity*, Quant. Struct. Act. Relat. 20 (2002), pp. 402–413.

[40] D. Case, T. Darden, T. Cheatham, C. Simmerling, J. Wang, R. Duke, R. Luo, M. Crowley, R.C. Walker, W. Zhang, K. Merz, B. Wang, S. Hayik, A. Roitberg, G. Seabra, I. Kolossvry, K.F. Wong, F. Paesani, J. Vanicek, X. Wu, S. Brozell, T. Steinbrecher, H. Gohlke, L. Yang, C. Tan, J. Mongan, V. Hornak, G. Cui, D. Mathews, M. Seetin, C. Sagui, V. Babin, and P. Kollman, *AMBER 10*, University of California, San Francisco, CA, 2008.

[41] W.L. Jorgensen, J. Chandrasekhar, J.D. Madura, R.W. Impey, and M.L. Klein, *Comparison of simple potential functions for simulating liquid water*, J. Chem. Phys. 779 (1983), pp. 926–935.

[42] T. Darden, D. York, and L. Pedersen, *Particle mesh Ewald: An Nlog(N) method for Ewald sums in large systems*, J. Chem. Phys. 98 (1993), pp. 10089–10092.

[43] R.W. Hockney, S.P. Goel, and J. Eastwood, *Quit high resolution computer models of plasma*, J. Comput. Phys. 14 (1974), pp. 148–158.

[44] B.P. Uberuaga, M. Anghel, and A.F. Voter, *Synchronization of trajectories in canonical molecular-dynamics simulations: Observation, explanation, and exploitation*, J. Chem. Phys. 120 (2004), pp. 6363–6374.

[45] D.J. Sindhikara, S. Kim, A.F. Voter, and A.E. Roitberg, *Bad seeds sprout perilous dynamics: Stochastic thermostat induced trajectory synchronization in biomolecules*, J. Chem. Theory Comput. 5 (2009), pp. 1624–1631.

[46] B. Hess, H. Bekker, H.J.C. Berendsen, and J.G.E.M. Fraaije, *LINCS: A linear constraint solver for molecular simulations*, J. Comput. Chem. 18 (1997), pp. 1463–1472.

[47] H.J.C. Berendsen, J.P.M. Postma, W.F. Vangunsteren, A. Dinola, and J.R. Haak, *Molecular-dynamics with coupling to an external bath*, J. Chem. Phys. 81 (1984), pp. 3684–3690.

[48] M. Parrinello and A. Rahman, *Polymorphic transitions in single crystals: A new molecular dynamics method*, J. Appl. Phys. 52 (1981), pp. 7182–7190.

[49] K.A. Sharp and B. Honig, *Electrostatic interactions in macromolecules: Theory and applications*, Annu. Rev. Biophys. Biophys. Chem. 19 (1990), pp. 301–332.

[50] N.A. Baker, D. Sept, S. Joseph, M.J. Holst, and J.A. McCammon, *Electrostatics of nanosystems: Application to microtubules and the ribosome*, Proc. Natl. Acad. Sci. USA 98 (2001), pp. 10037–10041.

[51] A. Shrake and J.A. Rupley, *Environment and exposure to solvent of protein atoms–lysozyme and insulin*, J. Mol. Biol. 79 (1973), pp. 351–371.

[52] D. Sitkoff, K.A. Sharp, and B. Honig, *Accurate calculation of hydration free energies using macroscopic solvent models*, J. Phys. Chem. 97 (1994), pp. 1978–1988.

[53] D.A. McQuarrie, *Statistical Thermodynamics*, 2nd ed., Harper and Row, New York, 1973.

[54] E.K. Ryu, Y.S. Choe, K.H. Lee, Y. Choi, and T. Kim, *Curcumin and dehydrozingerone derivatives: Synthesis, radiolabeling, and evaluation for beta-amyloid plaque imaging*, J. Med. Chem. 49 (2006), pp. 6111–6119.

[55] D. Kozakov, D.R. Hall, D. Beglov, R. Brenke, S.R. Comeau, Y. Shen, K. Li, J. Zheng, P. Vakili, I.C. Paschalidis, and S. Vajda, *Achieving reliability and high accuracy in automated protein docking: Cluspro, PIPER, SDU, and stability analysis in CAPRI rounds*, Proteins 78 (2010), pp. 3124–3130.

[56] D. Kozakov, R. Brenke, S.R. Comeau, and S. Vajda, *An FFT-based protein docking program with pairwise potentials*, Proteins 65 (2006), pp. 392–406.

[57] S.R. Comeau, D.W. Gatchell, S. Vajda, and C.J. Camacho, *ClusPro: An automated docking and discrimination method for the prediction of protein complexes*, Bioinformatics 20 (2004), pp. 45–50.

[58] S.R. Comeau, D.W. Gatchell, S. Vajda, and C.J. Camacho, *ClusPro: A fully automated algorithm for protein-protein docking*, Nucleic Acids Res. 32 (2004), pp. W96–W99.